Bone Reports 8 (2018) 95–103

Contents lists available at ScienceDirect

Bone Reports

journal homepage: www.elsevier.com/locate/bonr

Differential time-dependent transcriptional changes in the osteoblast lineage in cortical bone associated with sclerostin antibody treatment in ovariectomized rats

Scott Taylor[a], Rong Hu[a], Efrain Pacheco[a], Kathrin Locher[a], Ian Pyrah[a,1], Michael S. Ominsky[b,2], Rogely Waite Boyce[a,*]

[a] Department of Comparative Biology and Safety Sciences, Amgen Inc., One Amgen Center Drive, Thousand Oaks, CA 91320, USA
[b] Department of CardioMetabolic Disorders, Amgen Inc., One Amgen Center Drive, Thousand Oaks, CA 91320, USA

ARTICLE INFO

Keywords:
Osteoporosis
Therapeutics
Anabolics
Wnt signaling
Bone

ABSTRACT

Inhibition of sclerostin with sclerostin antibody (Scl-Ab) results in stimulation of bone formation on cancellous (Cn), endocortical (Ec), and periosteal (Ps) surfaces in rodents and non-human primates. With long-term dosing of Scl-Ab, the increase in bone formation is not sustained, attenuating first on Cn surfaces and later on Ec and Ps surfaces. In Cn bone, the attenuation in bone formation (self-regulation) is associated with transcriptional changes in the osteocyte (OCy) that would limit mitogenesis and are sustained with continued dosing. The expression changes in Cn OCy occur coincident with a decrease in osteoprogenitor (OP) numbers that may directly or indirectly be a consequence of the transcriptional changes in the OCy to limit OP proliferation. To characterize the Scl-Ab–mediated changes in cortical (Ct) bone and compare these changes to Cn bone, densitometric, histomorphometric, and transcriptional analyses were performed on femur diaphyses from aged ovariectomized rats. Animals were administered 50 mg/kg/wk of Scl-Ab or vehicle for up to 6 months (183 days), followed by a treatment-free period (up to 126 days). Scl-Ab increased Ct mass and area through day 183, which declined slightly when treatment was discontinued. Ps and Ec bone formation was sustained through the dosing on both Ct surfaces, with evidence of a decline in bone formation only at day 183 on the Ec surface. This is in contrast to Cn bone, where reduced bone formation was observed after day 29. TaqMan analysis of 60 genes with functional roles in the bone using mRNA isolated from laser capture micro-dissection samples enriched for Ec osteoblasts and Ct OCy suggest a pattern of gene expression in Ct bone that differed from Cn, especially in the OCy, and that corresponded to observed differences in the timing of phenotypic changes. Notable with Scl-Ab treatment was a "transcriptional switch" in Ct OCy at day 183, coincident with the initial decline in bone formation on the endocortex. A consistent sustained increase of expression for most genes in response to Scl-Ab was observed from day 8 through day 85 at the times of maximal bone formation on both Ct surfaces; however, at day 183, this increase was reversed, with expression of these genes generally returning to control values or decreasing compared to vehicle. Genes exhibiting this pattern included Wnt inhibitors *Sost* and *Dkk1*, though both had been up-regulated until the end of dosing in Cn OCy. Changes in cell cycle genes such as *Cdkn1a* and *Ndrg1* in Ct OCy suggested up-regulation of p53 signaling, as observed in Cn OCy; however, unlike in Cn bone, p53 signaling was not associated with decreased bone formation and was absent at day 183, when bone formation began to decline on the Ec surface. These data demonstrate involvement of similar molecular pathways in Ct and Cn bone in response to Scl-Ab but with a different temporal relationship to bone formation and

Abbreviations: ANOVA, analysis of variance; BMC, bone mineral content; BMP, bone morphogenetic protein; BS, bone surface; Cn, cancellous; Ct, cortical; Ec, endocortical; Ec.Pm, endocortical perimeter; LC, lining cells; LCM, laser capture micro-dissection; MS/BS, mineralizing surface; OB, osteoblast(s); OCy, osteocyte(s); OP, osteoprogenitor(s); OPG, osteoprotegerin; OVX, ovariectomized; pQCT, peripheral quantitative computed tomography; Ps, periosteal; Ps.Pm, periosteal perimeter; RANKL, receptor activator of nuclear factor kappa-B ligand; s.c., subcutaneous; Scl-Ab, sclerostin antibody; Scl-AbVI, 50 mg/kg of a Scl-Ab; TFP, treatment-free period; TGF, transforming growth factor; TP, treatment period; VEH, vehicle

* Corresponding author at: Department of Comparative Biology and Safety Sciences, Amgen Inc., One Amgen Center Drive, MS 29-2-A, Thousand Oaks, CA 91320, USA.
E-mail addresses: ssttaayy@gmail.com (S. Taylor), simplyrong@gmail.com (R. Hu), epacheco@amgen.com (E. Pacheco), kathrinl@amgen.com (K. Locher), ipyrah@seagen.com (I. Pyrah), ominsky@umich.edu (M.S. Ominsky), rboyce@amgen.com (R.W. Boyce).
[1] Current address: Seattle Genetics, 21823-30th Drive S.E., Bothell, WA 98021, USA.
[2] Current address: Radius Health, Inc., 950 Winter St., Waltham, MA 02451, USA.

https://doi.org/10.1016/j.bonr.2018.03.002
Received 26 October 2017; Received in revised form 15 February 2018; Accepted 13 March 2018
Available online 15 March 2018

suggest that the specific mechanism underlying self-regulation of Scl-Ab–induced bone formation may be different between Cn and Ct bone.

1. Introduction

As a consequence of inhibiting sclerostin and activating canonical Wnt signaling (Gong et al., 2016), sclerostin antibody (Scl-Ab) stimulates bone formation, decreases bone resorption, and increases bone mass and strength in both animals and humans (Cosman et al., 2016; Keaveny et al., 2015; McClung et al., 2014; Ominsky et al., 2017a; Ominsky et al., 2017b). The rapid increases in bone formation with Scl-Ab have been associated with the activation of bone lining cells (LC) and stimulation of modeling-based bone formation on cortical (Ct) and cancellous (Cn) bone surfaces (BS) (Boyce et al., 2017; Kim et al., 2017; Ominsky et al., 2014). The stimulation of modeling-based bone formation by Scl-Ab is transient. With long-term Scl-Ab administration, the attenuation (self-regulation) of bone formation exhibits bone surface-specific behavior. In previous rat and non-human primate studies with chronic administration of Scl-Ab, self-regulation of bone formation consistently occurs first on Cn surfaces followed by Ct surfaces (Chouinard et al., 2016; Li et al., 2014; Ominsky et al., 2017a; Ominsky et al., 2017b), underscoring the surface-specific response of bone formation in response to Scl-Ab.

The molecular basis for the self-regulation and surface-specific temporal behavior of bone formation in response to Scl-Ab is unknown. We have previously investigated the downstream signaling events associated with both the acute increase and self-regulation of bone formation in vertebral Cn bone of aged ovariectomized (OVX) rats administered Scl-Ab. Using laser capture micro-dissection (LCM) to enrich for subpopulations of the osteoblast (OB) lineage, we demonstrated that the acute downstream signaling in vivo in response to Scl-Ab involves up-regulation of selected canonical Wnt target genes coincident with the up-regulation of extracellular matrix genes in all mature OB subpopulations, i.e., OB, LC, and osteocytes (OCy) (Nioi et al., 2015). With long-term treatment, a “transcriptional switch” was observed in the Cn OCy at the time of peak bone formation, and this effect continued as bone formation declined during treatment. Transcriptional changes included alterations in the pattern of canonical Wnt gene expression and regulation of signaling pathways that would inhibit cell cycle progression (notably p53) and mitogenesis (notably c-Myc). Concurrent with these expression changes was a reduction in osteoprogenitor (OP) numbers. OCy signaling may be an example of transcriptional plasticity, the OCy simply mirroring the transcriptional response of OP to Scl-Ab. However, the observation that transcriptional signaling that limits mitogenesis occurs coincident with the initial reduction in OP number and the data demonstrating that this sustained transcriptional response is associated with progressive decrease in OP number suggest that these events likely contribute to self-regulation and progressive attenuation of bone formation with chronic Scl-Ab treatment. We hypothesized that Wnt signaling and downstream regulation of pathways that would inhibit cell cycle progression and mitogenesis in the OCy are potentially communicated to the OP population, perhaps by micro-vesicle transfer, to limit OP proliferation (Taylor et al., 2016).

The transcriptional profile in Ct bone in response to Scl-Ab and the relationship of gene expression changes with the delayed onset of self-regulation in Ct bone formation rates have not been investigated. In the current study, we have applied the same enrichment methods to subpopulations of the OB lineage from the mid-femur cortex and used a focused approach analyzing a selection of genes across several biological functions to examine the time-dependent transcriptional responses to acute and long-term Scl-Ab treatment in Ct bone, in order to gain a better understanding of the association of these responses with changes in Ct bone formation and bone mass and to relate the molecular changes to those previously reported for Cn bone.

2. Materials and methods

2.1. Study design

The study design has been previously presented (Taylor et al., 2016), and Ct analyses were limited to the vehicle (VEH) and Scl-Ab 50 mg/kg (Scl-AbVI) groups. The 3 mg/kg group was not included in this analysis because transcriptional changes were more robust at 50 mg/kg. Briefly, 6-month-old female Sprague Dawley rats (SD®IGS; Charles River Laboratories, Hollister, CA) were OVX and left untreated for 8 weeks, then administered by subcutaneous (s.c.) injection a VEH or Scl-AbVI (rat Fc construct) once weekly during a treatment period (TP) lasting through day 183. Up to 15 rats per group were euthanized at days 8, 29, 85, and 183. To assess the effects following treatment withdrawal, additional groups were maintained through a treatment-free period (TFP), and up to nine rats per group were euthanized at days 237 and 309 from the VEH and Scl-AbVI groups. For euthanasia, animals were anesthetized with isoflurane/oxygen and then exsanguinated.

Calcein green (10 mg/kg calcein green in 2% sodium bicarbonate in saline) was administered s.c. 13 and 3 days prior to scheduled euthanasia to label active bone-forming surfaces for dynamic histomorphometry and to facilitate active OB enrichment during LCM as described by Nioi et al. (2015). At necropsy, the left femur was collected for histomorphometry and peripheral quantitative computed tomography (pQCT) analyses of the mid-shaft. The right femur was collected for RNA analysis and cleaned of soft tissue; a 0.5–1 cm segment of cortex centered at the mid-shaft was isolated and embedded longitudinally in Tissue-Tek® O.C.T. (Sakura Finetek, Torrance, CA) in Peel-A-Way® disposable histology molds (Ted Pella, Inc., Redding, CA), snap frozen in liquid nitrogen, and stored at −80 °C until sectioning.

Animals were cared for in accordance with the *Guide for the Care and Use of Laboratory Animals*, 8th edition (National Research Council (US) Committee for the Update of the Guide for the Care and Use of Laboratory Animals, 2011). All research protocols were approved by the institutional animal care and use committee. Animals were group-housed (two per cage) at an internationally accredited Association for Assessment and Accreditation of Laboratory Animal Care facility in non-sterile, ventilated, micro-isolator housing with corn cob bedding. Animals had ad libitum access to pelleted feed (Rodent Diet 2020X; Teklad Diets, Madison, WI) and water (reverse osmosis purified) via an automatic watering system. Animals were maintained on a 12:12 h light:dark cycle in rooms with controlled temperature (72 °F ± 2 °F) and humidity (30%–70%) and had access to enrichment opportunities (Nylabones and Rat Retreats or Rat Tunnels).

2.2. Histomorphometry and pQCT

Left femurs were fixed in 70% ethanol, then scanned and analyzed on a Stratec XCT Research M instrument (Norland Medical Systems, Fort Atkinson, WI, software version 5.40). The length of the femur was measured with precision calipers, and a cross-sectional scan of the diaphysis was performed at 50% of the length from distal end of the bone at a voxel size of 0.1 mm. Ct bone was defined and analyzed using contour mode 2 and Ct mode 4. An outer threshold of 340 mg/cm^3 was used to distinguish the cortex from soft tissue. Following pQCT scanning, the mid-shaft was isolated using a Dremel MotoTool (Dremel, Mount Prospect, IL) and processed un-decalcified in polyester resin (Tap Plastics, San Jose, CA). Transverse cross-sections (approximately 150 µm thick) of femur cortex were taken using an Isomet low-speed saw (Buehler, Lake Bluff, IL) at approximately 50% of the femur length

and were ground to approximately 50 μm for analyses. Endocortical (Ec) and periosteal (Ps) labeled perimeters (L.Pm; i.e., Ec.L.Pm and Ps.L.Pm, respectively) were determined using an Osteomeasure system (OsteoMetrics, Decatur, GA).

For statistical analysis, a two-way analysis of variance (ANOVA) was performed across the two treatments, with a Sidak's post hoc test for comparisons with VEH (GraphPad Prism® version 6.05; GraphPad Software, Inc., La Jolla, CA, USA). Significance was set to the level of $p \leq 0.05$.

2.3. LCM, RNA extraction, TaqMan, and microarray

Cryosection preparation, LCM procedure and validation of cell enrichment, RNA extraction and amplification, and TaqMan assay were performed as previously described (Nioi et al., 2015). Briefly, LCM was performed on 4–6 μm cryosections of right femur diaphysis sectioned in the longitudinal axis from three animals per treatment group per time point to enrich for Ec OB and Ct OCy subpopulations for transcriptional analyses using TaqMan on a panel of key genes. Gene selection was guided by transcriptional changes observed in Cn bone and spanned a range of biological functions based on the Gene Ontology classification of biological processes and literature review. For convenience, these genes have been organized into groups of Wnt signaling, transforming growth factor (TGF)/bone morphogenetic protein (BMP) signaling, bone formation, bone resorption, cell cycle, and "other", though specific genes often have multiple or alternate functions in bone. Changes in expression were normalized using the average of the three housekeeping genes (*B2m*, *Hprt1*, and *Tbp*). Presence of fluorochrome

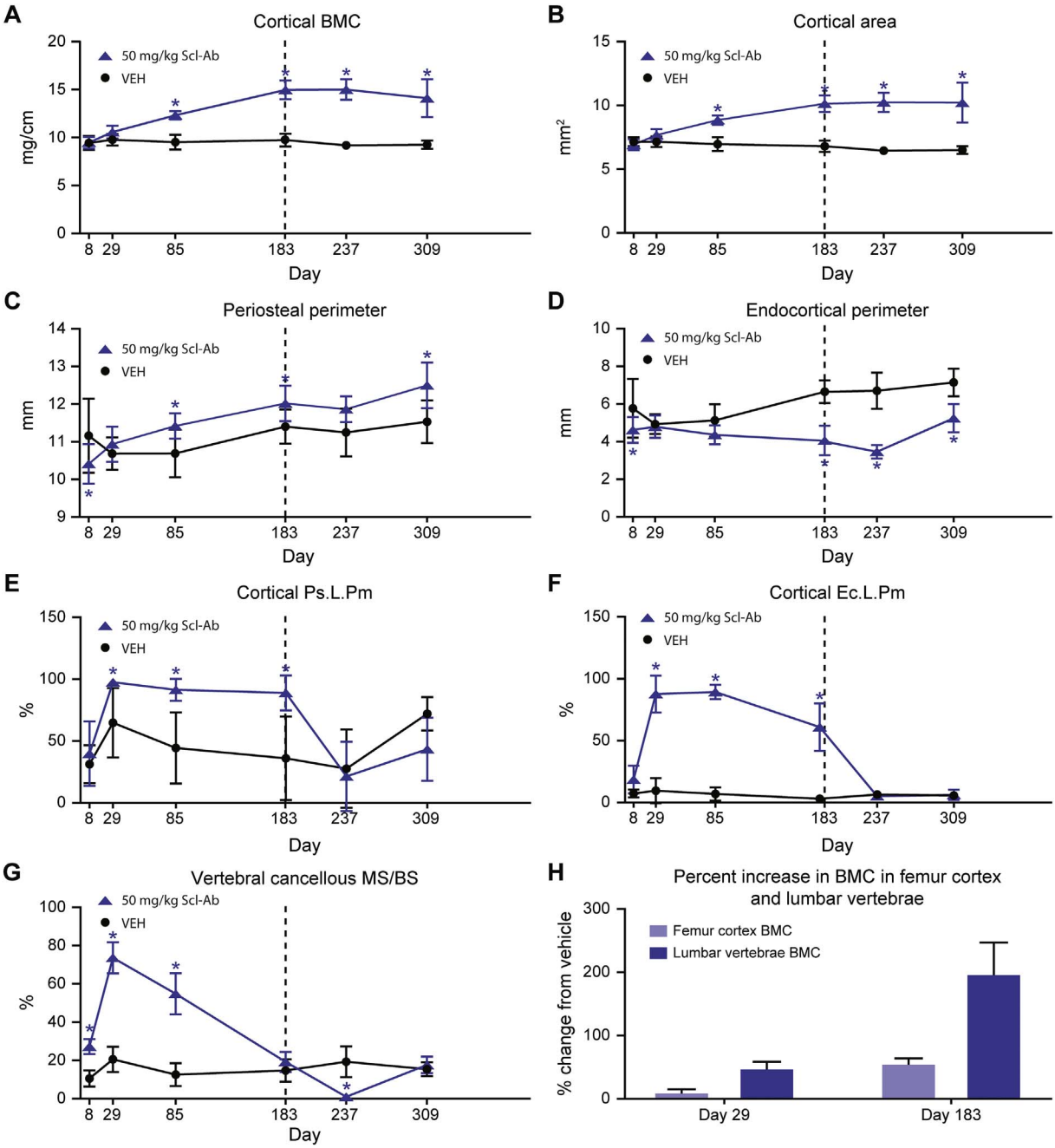

Fig. 1. Effect of Scl-Ab treatment on cortical bone formation and mass. (A) Cortical volumetric BMC. (B) Cortical area. (C) Periosteal perimeter. (D) Endocortical perimeter. (E) Cortical Ps.L.Pm. (F) Cortical Ec.L.Pm. (G) Vertebral cancellous MS/BS. (H) Percent change in BMC. Data are mean ± standard deviation. *$p \leq 0.05$. Vertical dotted line separates the TP on the left from the TFP on the right.

labeling was used to identify surfaces for enrichment of Ec OB and the entire Ct area was micro-dissected, avoiding the Ps and Ec surfaces, to enrich for OCy. Ps OB could not be consistently obtained due to the inadvertent stripping of the periosteum during removal of the soft tissue on several specimens, and therefore, were not included in the analyses. The RNA quality was good, with median RNA integrity number values ranging from 7.2 to 7.6 across all time points for both cell types. Statistical analyses were undertaken using the R statistical computing platform (version 3.1.0). Within a cell type, each gene was analyzed with a two-way ANOVA of treatment plus time (no interactions). Two-way ANOVA of bone type plus time was applied to Scl-Ab vs. VEH ratios to identify genes with different responses between Ct and Cn bone. In the comparison between bone types, input was limited to genes present in both Ct and Cn data sets and that were differentially expressed in response to Scl-Ab in one or both types of the bone. Welch *t*-test was used to compare Scl-Ab treatment to VEH control at individual time points. The criterion used for filtering and statistical significance was ANOVA $p \leq 0.05$. The complete set of summarized TaqMan results is provided in the Supplementary Material.

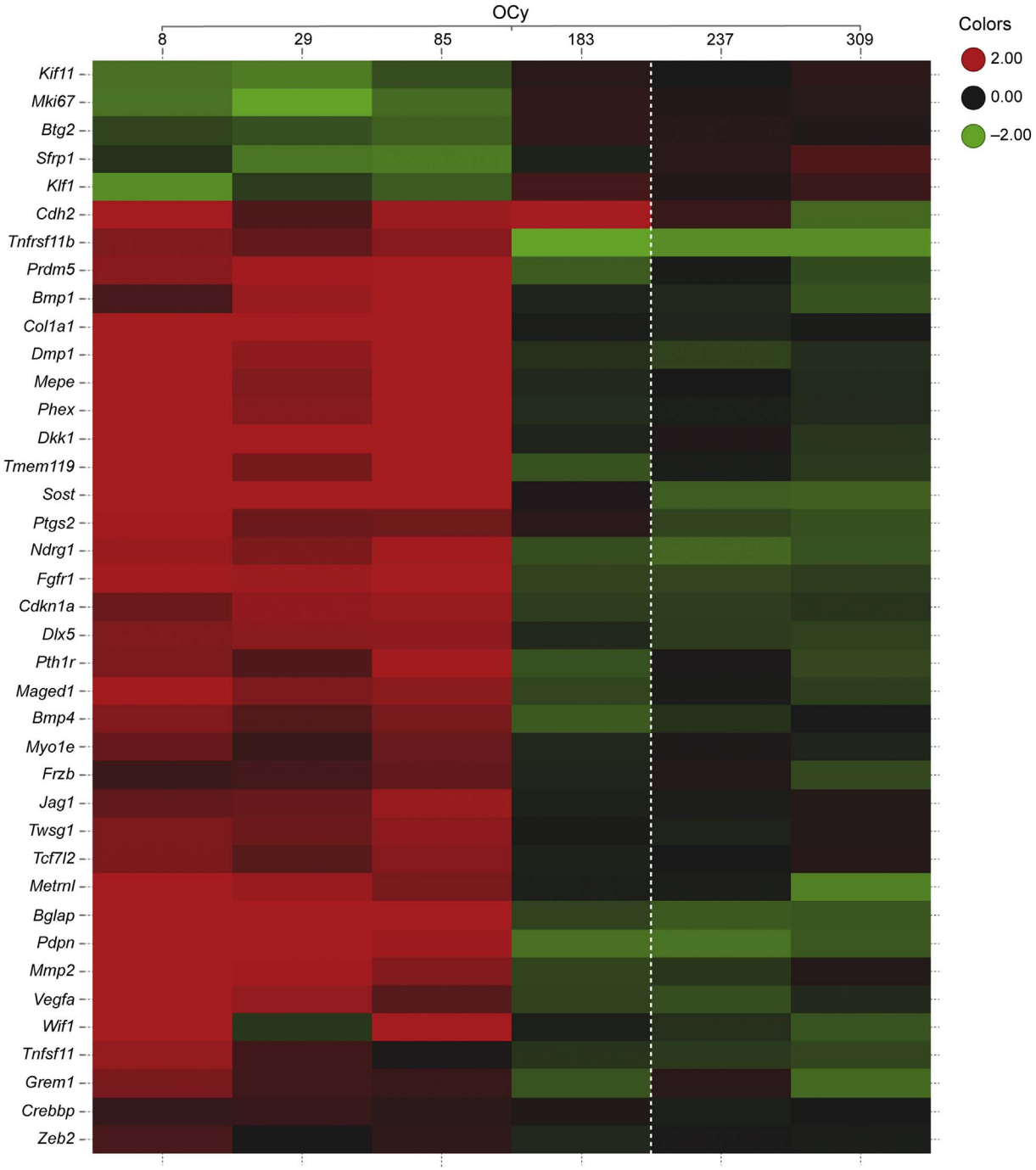

Fig. 2. Transcriptional changes by TaqMan in Ct OCy from Scl-Ab–treated rats. Rows are genes (hierarchical clustered) and columns are group-level responses to 50 mg/kg Scl-Ab (ordered by time point). $p \leq 0.05$ for each gene. Each cell contains the color-coded average log2 ratio of treatment vs. VEH control. The dotted vertical line separates the TP from the TFP. Values are capped at ± 2 (i.e., ± 4-fold change).

3. Results

3.1. Effects of Scl-Ab on Ct bone mass and formation

Scl-Ab resulted in significant increases in Ct volumetric bone mineral content (BMC) (Fig. 1A) and area (Fig. 1B) at day ≥85. The increase in Ct bone mass was associated with increased Ps perimeter (Ps.Pm) at day ≥85 (Fig. 1C) and decreased Ec perimeter (Ec.Pm) at day ≥183 (Fig. 1D). Ps.Pm and Ec.Pm were significantly decreased compared to VEH at day 8, which was considered spurious due to the short TP. The increases in Ps.Pm and decreases in Ec.Pm corresponded with significant increases in the surface extent of bone formation, Ps.L.Pm and Ec.L.Pm, at day 29 (Fig. 1E, F). The increase in Ps.L.Pm was sustained through day 183, with Ec.L.Pm beginning to decline at day 183. Ps.L.Pm and Ec.L.Pm returned to control levels in the TFP. It's worth noting that a site-specific response was also observed in a 12-month Scl-Ab dosing study in which Ec circumference did not increase in OVX rats from months 6 to 12 with weekly Scl-AbVI, while Ps circumference continued to expand during the same time period (unpublished Amgen internal data). This is in contrast to the pattern in vertebral Cn mineralizing surface (MS/BS) that peaked at day 29 and progressively declined to control values at day 183; in the TFP, MS/BS transiently decreased to essentially 0 at day 237, returning to baseline at day 309 (Fig. 1G). Scl-Ab resulted in greater bone mass accrual in the lumbar vertebrae, reaching an approximate increase of 200% in total BMC at day 183, compared with an approximate increase of only 50% in femur diaphysis relative to the mean of concurrent VEH controls (Fig. 1H).

3.2. Time-dependent transcriptional changes in Ct OCy in response to Scl-Ab

Successful enrichment of OB and OCy subpopulations was confirmed by analyzing expression in VEH control samples of typical OB- and OCy-related genes (Supplementary Fig. 1). The transcriptional response to Scl-Ab in Ec OB (Supplementary Figs. 2, 3) generally followed a pattern expected from OB actively forming new bone with genes showing a steady pattern of regulation throughout the TP, consistent with the sustained high level of bone formation.

In Ct OCy, there was a notable consistent pattern of expression at days 8–85, with a prominent directional switch in gene expression at day 183 that was generally sustained through the TFP (Fig. 2). Genes related to Wnt signaling and bone formation were robustly up-regulated at days 8–85, with their subsequent expression generally returning to control levels or below at days 183–309. This included up-regulation of the Wnt target genes *Vegfa* and *Mmp2*, and the extracellular Wnt inhibitors *Sost* and *Dkk1*. In addition, *Tcf7l2*, also a negative regulator of canonical Wnt signaling (Tang et al., 2008), was up-regulated following a similar pattern. Another Wnt signaling modulator, *Sfrp1*, was decreased at days 8–85 before returning toward VEH-treated levels at day 183. Interestingly, *Cdh2*, a gene that has been shown to interfere with the activity of the Wnt/β-catenin pathway (Marie et al., 2014)

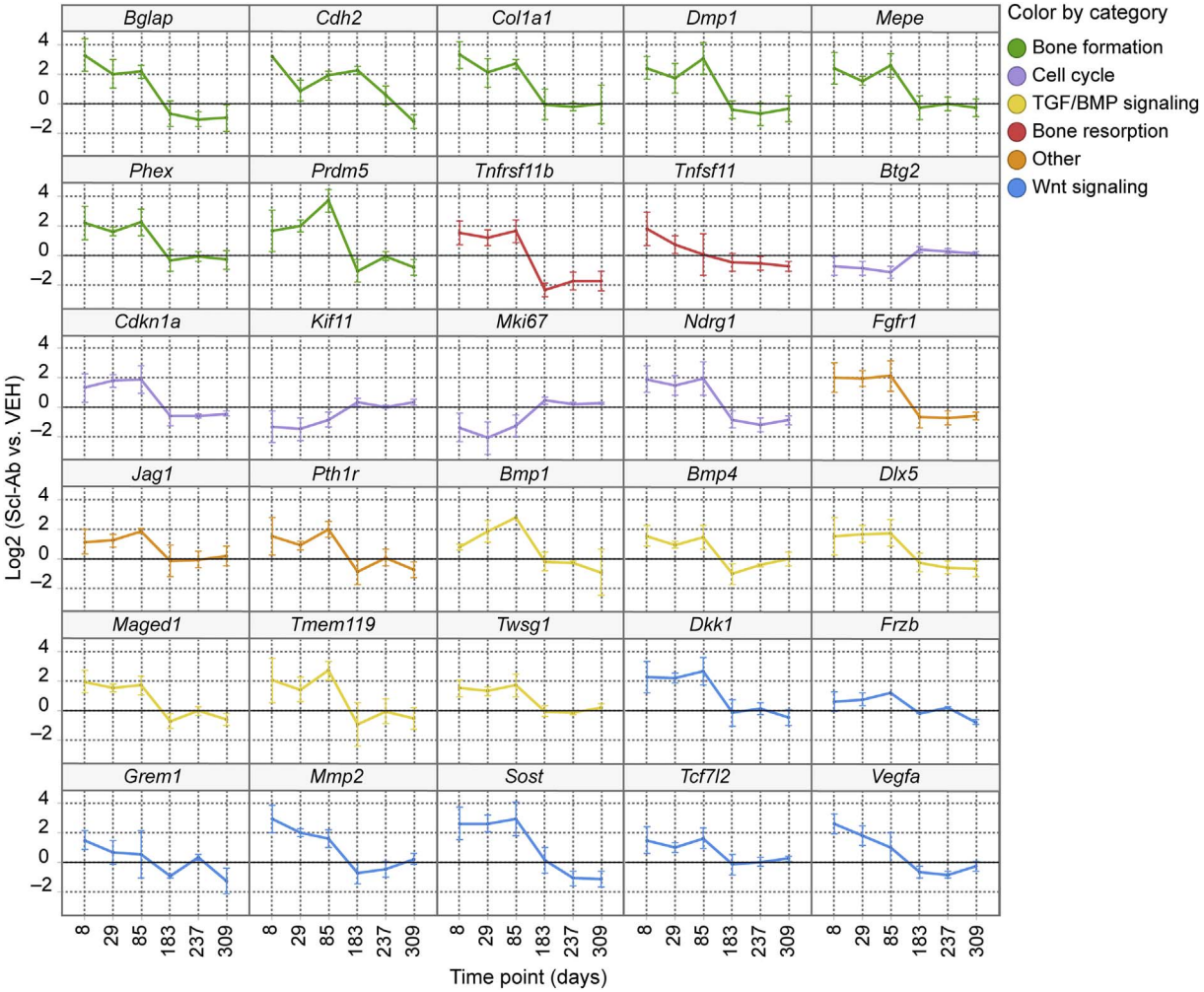

Fig. 3. Expression changes of selected genes in Ct OCy collected from rats treated with Scl-AbVI. Genes had measured expression values for all biological replicates and $p \leq 0.05$. Data are mean ± standard error of the mean. Genes are grouped by their biological function.

remained increased at day 183 in contrast to other Wnt-related genes. Genes related to bone formation, matrix synthesis, and mineralization, including *Postn* ($p = 0.06$), a Wnt target gene that promotes Ps bone formation (Bonnet et al., 2017), as well as genes related to TGFβ/BMP signaling (*Dlx5*, *Twsg1*, *Bmp4*, *Fgfr1*, and *Pth1r*) and genes related to motility (*Pdpn* and *Myo1e*) generally followed the same pattern as the Wnt signaling and bone-formation genes. *Bglap* and *Col1a1*, genes typically associated with OB, were up-regulated in OCy as has been seen in Cn OCy (Nioi et al., 2015; Taylor et al., 2016).

Genes with known roles related to cell cycle and regulated by Scl-Ab suggest an anti-mitogenic signal at days 8–85. The p53 target genes *Ndrg1* and *Cdkn1a* (p21) along with *Maged1*, a regulator of *Dlx5* with anti-proliferative effects on the OB lineage (Liu et al., 2015), and *Prmd5*, a gene reported to promote cell cycle arrest (Deng and Huang, 2004), were up-regulated at days 8–85 and then generally down-regulated at days 183–309. Pro-mitotic genes such as *Kif11* and *Mki67* were decreased at days 8–85 and then returned to control values at days 183–309. In contrast, *Btg2*, a p53 target with anti-proliferative activity, was down-regulated at days 8–85. The observed changes in expression of *Btg2* may relate more to its reported function as an enhancer of BMP signaling (Park et al., 2004). Time-dependent changes in expression of selected genes across biological functions in the Ct OCy in response to Scl-Ab are presented in Fig. 3.

Genes related to bone resorption that were significantly regulated by Scl-Ab include *Tnfsf11* (receptor activator of nuclear factor kappa-B ligand [RANKL]) and *Tnfrsf11b* (osteoprotegerin [OPG]); however, the two genes respond differently over time. OPG was up-regulated at days 8–85 and then down-regulated at day 183. RANKL was up-regulated at day 8 and trended downward during the TP and through the TFP. The RANKL/OPG ratio (Fig. 4) was not significantly different from VEH control except at day 183.

3.3. Differential expression of genes in response to Scl-Ab between Ct and Cn OCy

Previous experiments (Taylor et al., 2016) included TaqMan data for Cn OCy from Scl-Ab–treated rats at days 8, 183, and 309. The temporal pattern of genes profiled by TaqMan in both Cn and Ct OCy were compared at these time points for genes that overlapped between the two TaqMan panels and that were significantly altered by Scl-Ab treatment in at least one bone type (Supplementary Fig. 4). The temporal expression patterns of genes related to bone formation (*Bglap*, *Col1a*, and *Tmem119*) were generally similar in Cn and Ct OCy. However, a notable difference was the sustained increase in expression of p53 target genes (*Cdkn1a* and *Ndrg1*) in Cn OCy at day 183 when bone formation had returned to control values compared with the rapid normalization of expression of these genes in Ct OCy at day 183 when bone formation was beginning to decline (Fig. 5). Another p53 target and Wnt inhibitor important in bone, *Dkk1* ($p = 0.10$) (Niida et al., 2004), had a similar expression profile (Fig. 5). In addition, the key extracellular Wnt inhibitor *Sost* was up-regulated in Ct OCy during maximal bone formation at days 8–85 but normalized to control values once Ec bone formation was beginning to decline at day 183. This contrasts with Cn OCy, where expression of both *Dkk1* and *Sost* remained elevated through day 183 even though Cn bone formation had returned to control values.

4. Discussion

This study characterizes the time-dependent changes in femur Ct bone mass, bone formation, and transcriptional signaling in diaphyseal Ec OB and Ct OCy in OVX rats administered Scl-Ab for a 6-month TP, followed by a TFP. Ct bone mass and area progressively increased during the TP, associated with a sustained increase in bone formation on the Ps and Ec surfaces (with the exception of a decline only on the Ec

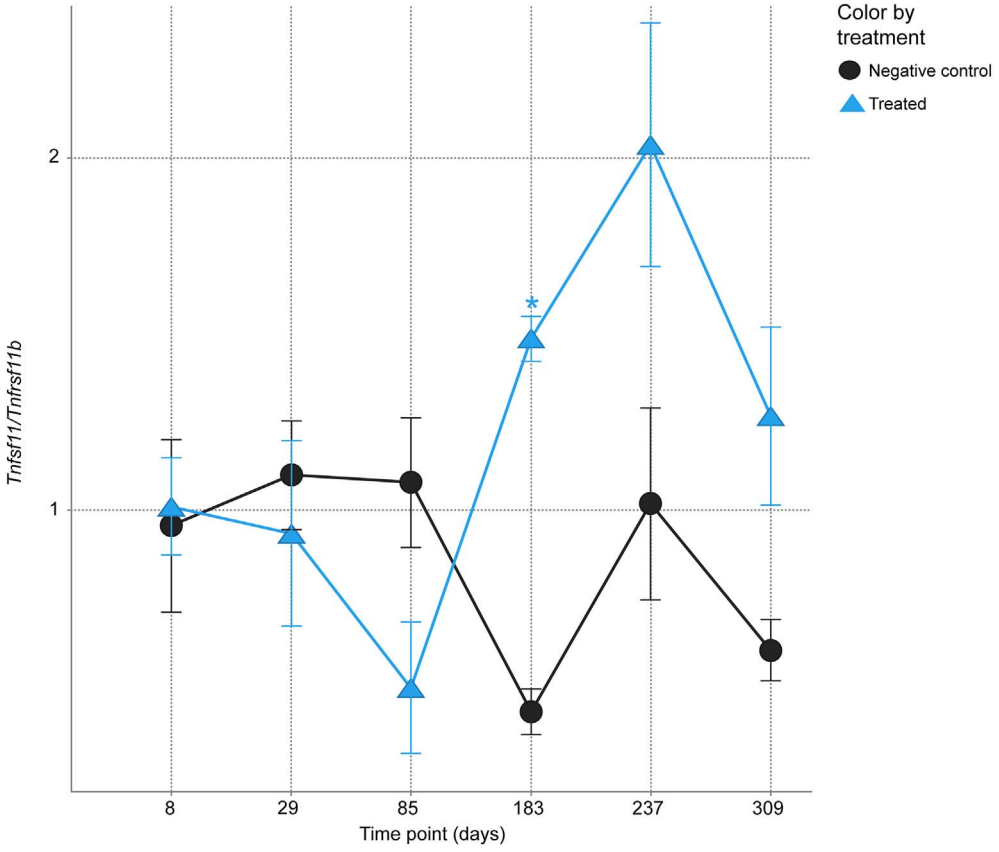

Fig. 4. Time-dependent RANKL/OPG ratio with Scl-AbVI in Ct OCy. Data are mean ± standard error of the mean. *t-test $p \leq 0.05$.

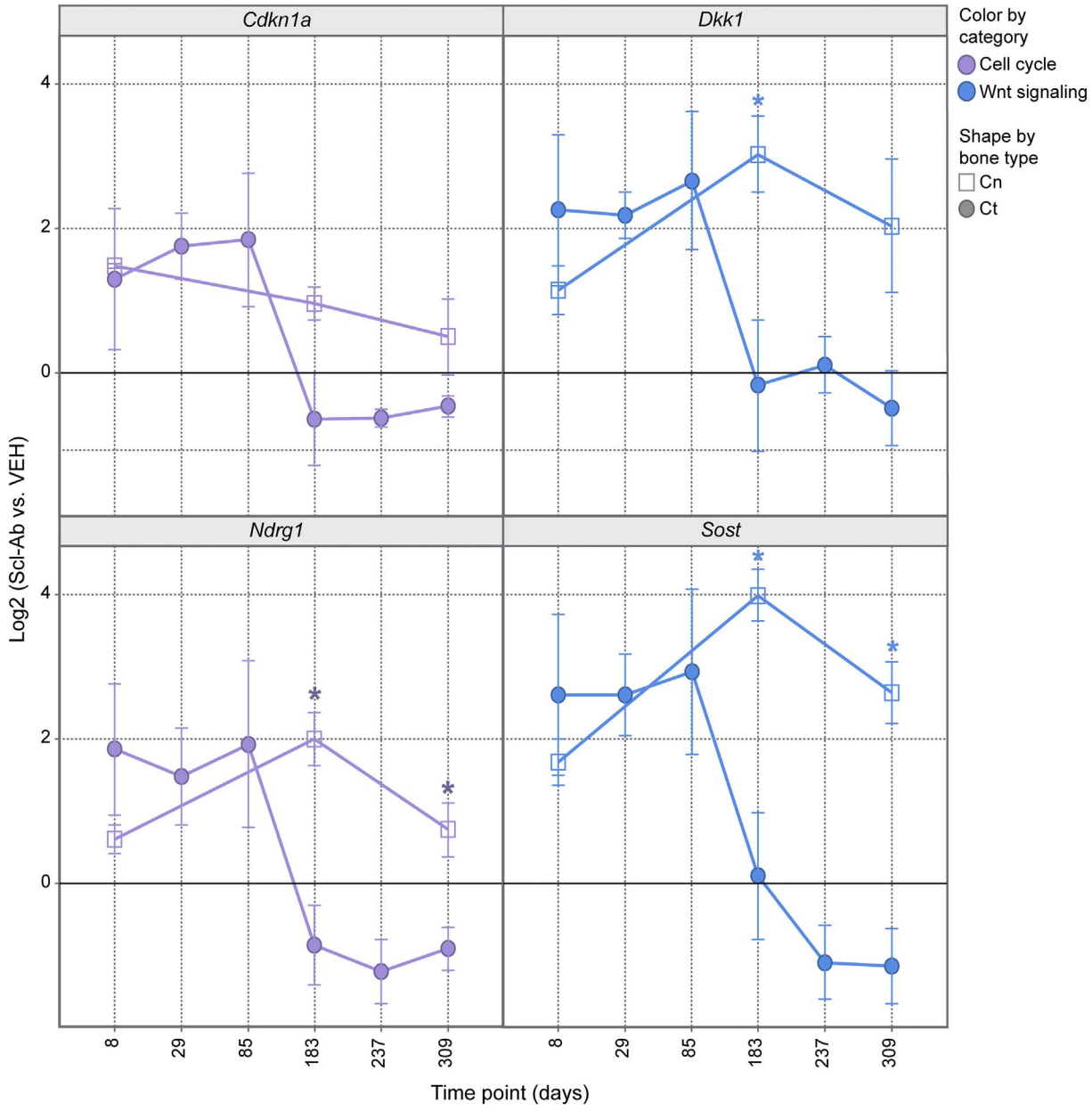

Fig. 5. Differential transcriptional response in rats treated with Scl-AbVI of selected p53 targets and Wnt inhibitors in Ct and Cn OCy. Shapes represent Ct OCy (circles) and Cn OCy (squares). Data are mean ± standard error of the mean. $p \leq 0.05$ (except *Dkk1* with $p = 0.10$).

surface at day 183). This is in contrast to Cn bone, where MS/BS peaked at day 29 and then self-regulated to control values by the end of the TP. The onset of self-regulation in Cn bone was temporally associated with transcriptional signaling in the Cn OCy, consistent with the inhibition of mitogenesis and progressive decreases in OP numbers (Taylor et al., 2016). In Cn bone, we hypothesize that signaling events downstream of canonical Wnt in OCy triggered a transcriptional response to limit mitogenesis of OP via marked up-regulation of p53 signaling and other tumor suppressor pathways downstream of c-Myc signaling, contributing to the progressive decrease in bone formation to control levels. The OCy transcriptional response may simply mirror the transcriptional changes in OP or the OCy may potentially communicate this transcriptional signal to the OP via a mechanism such as micro-vesicle transfer.

To investigate transcriptional changes in Ct bone and relate this response to the previously reported Cn response, a selected panel of genes was examined by TaqMan in femur Ec OB and Ct OCy that captured genes and pathways that were generally differentially regulated in Cn OCy by Scl-Ab. In Ec OB, expression changes were generally as expected from cells actively producing new bone. Expression of genes related to bone matrix was increased throughout the TP, consistent with histomorphometric data. Expression of some of these genes decreased slightly from their highest values in Ec OB at day 183, consistent with the slight attenuation of bone formation on the Ec surface. These observed changes in genes related to bone formation were gradual compared to the more dramatic decreases in similar genes in Cn OB that followed the onset of attenuation of Cn bone formation. In general, these changes returned to control levels by the end of the TFP.

In Ct OCy, changes in the expression of genes consistent with increased bone formation, increased Wnt and TGFβ/BMP signaling, and decreased mitogenesis were observed at days 8–85 when bone formation was maximal on Ct surfaces. However, at day 183 while still in the TP, increased expression values generally returned to control levels or were decreased relative to control, changes that were sustained through the TFP. This response suggests a “transcriptional switch” in the Ct OCy that was not observed in Ec OB and that temporally aligns with the

onset of attenuation of bone formation on the Ec surface. The normalization of gene expression values at day 183, including Wnt inhibitors, contrasts with Cn OCy, where changes in Wnt and downstream regulatory pathways remained differentially regulated through day 183, even though Cn bone formation had returned to control levels. This pattern extended to *Wisp1* ($p = 0.07$, Supplementary Fig. 5), a Wnt target with roles in both bone formation and resorption (Maeda et al., 2015), that was decreased in Ct OCy at day 183 though bone formation remained elevated but had displayed sustained up-regulation through the TP in Cn OCy even after Cn bone formation returned to baseline values.

Another notable difference between Cn and Ct OCy was the pattern of regulation of genes related to osteoclastogenesis. In Cn OCy, the pattern of regulation of differentially expressed genes with a critical role in osteoclastogenesis, including increased OPG resulting in decreased RANKL/OPG ratio, was consistent with inhibition of bone resorption that aligned with reduction in eroded surface. This pattern of regulation was sustained through the TP. In Ct OCy, there was no clear signal for inhibition of resorption. RANKL/OPG ratio was unchanged at days 8–85 despite the up-regulation of OPG following a similar pattern as other Wnt target genes *Vegfa* and *Mmp2*. Not until day 183, when OPG returned to control levels, did the resulting increase in RANKL/OPG suggest a pro-resorptive condition. A pro-resorptive signal during the TP with continued Scl-Ab exposure again highlights the distinctly different response in Ct bone vs. Cn bone.

In Ct bone, there was evidence of p53 signaling when bone formation was maximal on Ct surfaces at days 8–85 by the increased expression of hallmark targets of p53, such as *Ndrg1*, *Cdkn1a*, and *Dkk1* (el-Deiry et al., 1993; Niida et al., 2004; Stein et al., 2004). However, unlike Cn bone, increased expression of these known p53 target genes was not associated with attenuation of bone formation. At day 183, when Ec bone formation was beginning to decline, expression changes in these genes were normalized. This may suggest that p53 signaling in Ct bone in response to Scl-Ab perhaps works to govern bone formation when it is maximal, coordinating cell growth and cell proliferation rather than triggering the attenuation of Ct bone formation through cell cycle arrest (Vousden and Prives, 2009). Alternatively, p53 signaling may function to protect from cell stress (Green and Kroemer, 2009; Vousden and Lane, 2007). Unique signals temporally associated with initiation of the attenuation of Ct bone formation that may contribute to self-regulation were not evident from the TaqMan gene panel.

The return to control levels of many Wnt target genes and Wnt inhibitors in Ct OCy such as *Sost* and *Dkk1* before the end of dosing at day 183 was an unexpected finding. This is in contrast to the response in Cn OCy and may offer insight into potential mechanistic differences of self-regulation in Ct bone. In Ct OCy, up-regulation of genes consistent with Wnt inhibition and p53 activity returns toward baseline together at the same time when the first decrease in bone formation is observed on the Ec surface. Their continued up-regulation appears unnecessary to effect attenuation of bone formation. Extracellular Wnt inhibitors (*Sost* and *Dkk1*) as well as p53 signaling may function to moderate bone formation, rather than participate in triggering a complete shutdown. The molecular signaling responsible for initiating the attenuation of Ec bone formation was not evident from the TaqMan panel of genes. By comparison, up-regulation of genes consistent with Wnt inhibition and p53 activity in Cn OCy is sustained beyond the observed peak in Cn bone formation and persists as bone formation attenuates and approaches control levels. These observations suggest that these negative regulatory pathways play key roles in effecting the progressive attenuation of bone formation. It has been recently recognized that OCy from different skeletal sites display distinct transcriptional repertoires, which could support the concept of a differential response of Cn and Ct OCy to Scl-Ab (Youlten et al., 2017).

In conclusion, a progressive increase in femur Ct bone mass due to increased bone formation on Ec and Ps surfaces occurred in aged OVX rats treated with Scl-Ab for 6 months followed by a TFP. Bone formation remained high throughout the TP, showing a modest decline only on the Ec surface on day 183. TaqMan analyses of Ec OB highlighted activation of Wnt signaling and gene expression changes expected from OB actively synthesizing new bone matrix, consistent with the responses observed in Cn OB. In Ct OCy, a consistent pattern of gene expression across biological functions in response to Scl-Ab was observed at days 8–85, coinciding with maximal bone formation on Ct surfaces. However, at day 183, expression of these genes generally returned to control values coincident with the attenuation of bone formation on the Ec surface. The association of a transcriptional switch in Ct OCy corresponding to a decline in Ec bone formation at day 183 is similar to what was observed in Cn OCy, where changes in gene expression were coupled with self-regulation of Cn bone beginning at day 29. Affected genes included Wnt inhibitors that had remained up-regulated throughout the TP in Cn OCy. Changes in cell cycle genes suggested up-regulation of p53 signaling, similar to that observed in Cn OCy; however, these were not associated with attenuation of bone formation and were not sustained through the TP. The different pattern of expression of Wnt signaling and regulators of cell cycle such as p53 signaling and corresponding changes in bone formation suggest potentially different functions in Cn and Ct bone in response to Scl-Ab. In Cn bone, these regulators coincide with the onset of attenuation of bone formation and are sustained as bone formation is normalized to control levels, suggesting a more critical role in shutting down bone formation. In Ct bone, these regulators may operate to moderate bone formation at the times of maximal bone formation on Ct surfaces or are an adaptive response to cell stress, but they do not appear to trigger the onset of self-regulation. Although the current analysis provides important insight into the mechanism of action of Scl-Ab in Ct bone, further work is required to identify the specific molecular mechanisms responsible for triggering attenuation of Ct bone formation with continued administration.

Transparency document

The Transparency document associated with this article can be found in the online version.

Acknowledgments

The authors thank Drs. Thomas J. Wronksi and J. Ignacio Aguirre for performing the histomorphometric and densitometric analyses. The authors are grateful to Gurpreet Kaur of Cactus Communications (on behalf of Amgen Inc.) and Amy Foreman of Amgen Inc. for editing and formatting the manuscript; the Amgen CBSS staff, particularly Emily Frazier, Linda Cherepow, and Marnie Higgins-Garn, for conducting the in-life phase of this study; Yuan Chen for assistance with RNA extraction and amplification; Karen Hettwer for cryotomy support; Paul Nioi and Yudong He for helpful advice; and Drs. Ruth Lightfoot-Dunn and Cindy Afshari for their unwavering support. Stephanie Lachacz, Cameron Suarez, and Alyssa Williams from the University of Florida (Gainesville) provided expert technical assistance for bone histomorphometry.

Funding

This work was supported by Amgen Inc. and UCB Pharma.

Conflict of interest

ST, RH, EP, and KL are employees of Amgen Inc. and have Amgen Inc. stock and/or stock options. IP is a former Amgen employee and current employee of Seattle Genetics, Inc. and owns Seattle Genetics Inc. and AstraZeneca PLC stock. MSO is a former Amgen employee and currently employed at Radius Health, Inc. and owns Radius and Amgen Inc. stock. RWB is a former Amgen employee.

Author contributions

All authors participated in the design or implementation of the study and/or the analysis or interpretation of the findings and had access to the study data. All authors contributed to the development and critical revision of the manuscript and approved the final version for submission. ST and RWB take responsibility for the integrity of the data analysis.

Appendix A. Supplementary data

Supplementary data to this article can be found online at https://doi.org/10.1016/j.bonr.2018.03.002.

References

Bonnet, N., Brun, J., Rousseau, J.C., Duong, L.T., Ferrari, S.L., 2017. Cathepsin K controls cortical bone formation by degrading periostin. J. Bone Miner. Res. 32 (7), 1432–1441.

Boyce, R.W., Niu, Q.T., Ominsky, M.S., 2017. Kinetic reconstruction reveals time-dependent effects of romosozumab on bone formation and osteoblast function in vertebral cancellous and cortical bone in cynomolgus monkeys. Bone 101, 77–87.

Chouinard, L., Felx, M., Mellal, N., Varela, A., Mann, P., Jolette, J., Samadfam, R., Smith, S.Y., Locher, K., Buntich, S., Ominsky, M.S., Pyrah, I., Boyce, R.W., 2016. Carcinogenicity risk assessment of romosozumab: a review of scientific weight-of-evidence and findings in a rat lifetime pharmacology study. Regul. Toxicol. Pharmacol. 81, 212–222.

Cosman, F., Crittenden, D.B., Adachi, J.D., Binkley, N., Czerwinski, E., Ferrari, S., Hofbauer, L.C., Lau, E., Lewiecki, E.M., Miyauchi, A., Zerbini, C.A., Milmont, C.E., Chen, L., Maddox, J., Meisner, P.D., Libanati, C., Grauer, A., 2016. Romosozumab treatment in postmenopausal women with osteoporosis. N. Engl. J. Med. 375 (16), 1532–1543.

Deng, Q., Huang, S., 2004. PRDM5 is silenced in human cancers and has growth suppressive activities. Oncogene 23 (28), 4903–4910.

el-Deiry, W.S., Tokino, T., Velculescu, V.E., Levy, D.B., Parsons, R., Trent, J.M., Lin, D., Mercer, W.E., Kinzler, K.W., Vogelstein, B., 1993. WAF1, a potential mediator of p53 tumor suppression. Cell 75 (4), 817–825.

Gong, J., Cao, J., Ho, J., Chen, C., Paszty, C., 2016. Romosozumab blocks the binding of sclerostin to the two key Wnt signaling co-receptors, LRP5 and LRP6, but not to LRP4. http://www.asbmr.org/education/2016-abstracts, Accessed date: 19 March 2017.

Green, D.R., Kroemer, G., 2009. Cytoplasmic functions of the tumour suppressor p53. Nature 458 (7242), 1127–1130.

Keaveny, T., Crittenden, D., Bolognese, M., Genant, H., Engelke, K., Oliveri, B., Brown, J., Langdahl, B., Yang, Y., Grauer, A., Libanati, C., 2015. Strength at the lumbar spine and hip improves with romosozumab compared with teriparatide in postmenopausal women with low bone mass. Presented at: Annual Meeting of the American College of Rheumatology/Association of Rheumatology Health Professionals Annual Meeting; November 6–11, 2015; San Francisco, CA. Abstract 3175.

Kim, S.W., Lu, Y., Williams, E.A., Lai, F., Lee, J.Y., Enishi, T., Balani, D.H., Ominsky, M.S., Ke, H.Z., Kronenberg, H.M., Wein, M.N., 2017. Sclerostin antibody administration converts bone lining cells into active osteoblasts. J. Bone Miner. Res. 32 (5), 892–901.

Li, X., Niu, Q.T., Warmington, K.S., Asuncion, F.J., Dwyer, D., Grisanti, M., Han, C.Y., Stolina, M., Eschenberg, M.J., Kostenuik, P.J., Simonet, W.S., Ominsky, M.S., Ke, H.Z., 2014. Progressive increases in bone mass and bone strength in an ovariectomized rat model of osteoporosis after 26 weeks of treatment with a sclerostin antibody. Endocrinology 155 (12), 4785–4797.

Liu, M., Xu, L., Ma, X., Xu, J., Wang, J., Xian, M., Zhou, X., Wang, M., Wang, F., Qin, A., Pan, Q., Wen, C., 2015. MAGED1 is a negative regulator of bone remodeling in mice. Am. J. Pathol. 185 (10), 2653–2667.

Maeda, A., Ono, M., Holmbeck, K., Li, L., Kilts, T.M., Kram, V., Noonan, M.L., Yoshioka, Y., McNerny, E.M., Tantillo, M.A., Kohn, D.H., Lyons, K.M., Robey, P.G., Young, M.F., 2015. WNT1-induced secreted protein-1 (WISP1), a novel regulator of bone turnover and Wnt signaling. J. Biol. Chem. 290 (22), 14004–14018.

Marie, P.J., Hay, E., Modrowski, D., Revollo, L., Mbalaviele, G., Civitelli, R., 2014. Cadherin-mediated cell-cell adhesion and signaling in the skeleton. Calcif. Tissue Int. 94 (1), 46–54.

McClung, M.R., Grauer, A., Boonen, S., Bolognese, M.A., Brown, J.P., Diez-Perez, A., Langdahl, B.L., Reginster, J.Y., Zanchetta, J.R., Wasserman, S.M., Katz, L., Maddox, J., Yang, Y.C., Libanati, C., Bone, H.G., 2014. Romosozumab in postmenopausal women with low bone mineral density. N. Engl. J. Med. 370 (5), 412–420.

National Research Council (US) Committee for the Update of the Guide for the Care and Use of Laboratory Animals, 2011. Guide for the Care and Use of Laboratory Animals. National Academies Press (US), Washington, D.C.

Niida, A., Hiroko, T., Kasai, M., Furukawa, Y., Nakamura, Y., Suzuki, Y., Sugano, S., Akiyama, T., 2004. DKK1, a negative regulator of Wnt signaling, is a target of the beta-catenin/TCF pathway. Oncogene 23 (52), 8520–8526.

Nioi, P., Taylor, S., Hu, R., Pacheco, E., He, Y.D., Hamadeh, H., Paszty, C., Pyrah, I., Ominsky, M.S., Boyce, R.W., 2015. Transcriptional profiling of laser capture microdissected subpopulations of the osteoblast lineage provides insight into the early response to sclerostin antibody in rats. J. Bone Miner. Res. 30 (8), 1457–1467.

Ominsky, M.S., Niu, Q.T., Li, C., Li, X., Ke, H.Z., 2014. Tissue-level mechanisms responsible for the increase in bone formation and bone volume by sclerostin antibody. J. Bone Miner. Res. 29 (6), 1424–1430.

Ominsky, M.S., Boyce, R.W., Li, X., Ke, H.Z., 2017a. Effects of sclerostin antibodies in animal models of osteoporosis. Bone 96, 63–75.

Ominsky, M.S., Boyd, S.K., Varela, A., Jolette, J., Felx, M., Doyle, N., Mellal, N., Smith, S.Y., Locher, K., Buntich, S., Pyrah, I., Boyce, R.W., 2017b. Romosozumab improves bone mass and strength while maintaining bone quality in ovariectomized cynomolgus monkeys. J. Bone Miner. Res. 32 (4), 788–801.

Park, S., Lee, Y.J., Lee, H.J., Seki, T., Hong, K.H., Park, J., Beppu, H., Lim, I.K., Yoon, J.W., Li, E., Kim, S.J., Oh, S.P., 2004. B-cell translocation gene 2 (Btg2) regulates vertebral patterning by modulating bone morphogenetic protein/smad signaling. Mol. Cell. Biol. 24 (23), 10256–10262.

Stein, S., Thomas, E.K., Herzog, B., Westfall, M.D., Rocheleau, J.V., Jackson 2nd, R.S., Wang, M., Liang, P., 2004. NDRG1 is necessary for p53-dependent apoptosis. J. Biol. Chem. 279 (47), 48930–48940.

Tang, W., Dodge, M., Gundapaneni, D., Michnoff, C., Roth, M., Lum, L., 2008. A genome-wide RNAi screen for Wnt/beta-catenin pathway components identifies unexpected roles for TCF transcription factors in cancer. Proc. Natl. Acad. Sci. U. S. A. 105 (28), 9697–9702.

Taylor, S., Ominsky, M.S., Hu, R., Pacheco, E., He, Y.D., Brown, D.L., Aguirre, J.I., Wronski, T.J., Buntich, S., Afshari, C.A., Pyrah, I., Nioi, P., Boyce, R.W., 2016. Time-dependent cellular and transcriptional changes in the osteoblast lineage associated with sclerostin antibody treatment in ovariectomized rats. Bone 84, 148–159.

Vousden, K.H., Lane, D.P., 2007. p53 in health and disease. Nat. Rev. Mol. Cell Biol. 8 (4), 275–283.

Vousden, K.H., Prives, C., 2009. Blinded by the light: the growing complexity of p53. Cell 137 (3), 413–431.

Youlten, S., Baldock, P., Leitch, V., Quinn, J., Bartonicek, N., Chai, R., Eisman, J., Bassett, J.H.D., Williams, G., Croucher, P., 2017. Osteocytes express a unique transcriptome that underpins skeletal homeostasis. Presented at: Annual Meeting of the American Society for Bone and Mineral Research; September 8–11, 2017; Denver, CO.